Dynamic Positioning using Model Predictive Control with Short-Term Wave Prediction

Henning Øveraas*, Håkon S. Halvorsen*, Olav Landstad*, Vidar Smines**, Tor A. Johansen*, *Senior Member, IEEE*

Abstract

Remotely operated vehicle (ROV) operations are today typically supported by large designated vessels. New emerging concepts aims to streamline ROV operations by utilising unmanned surface vessels of a smaller size. Reduction in size may result in first-order wave induced motion being more significant. This motivates the use of dynamic positioning control using thrusters to actively compensate for first-order wave-driven horizontal-plane motion in order to maximise operability. This paper proposes a controller for dynamic positioning based on model predictive control and short-term wave motion prediction intended to actively compensate for first-order waves. By considering the full dynamic sea environment, the controller is able to dampen out some of the oscillatory motion caused by first-order waves. The controller is able reduce the average deviation from the set-point with up to 65% for a variety of sea conditions. The maximum distance error to the reference point is reduced by up to 65% depending on sea state. The dynamics of the thrusters is a limiting factor when counteracting first-order waves and fast thrusters are therefore crucial in achieving best possible positioning. The cost of the wave-compensated positioning is a more dynamic consumption of power.

Index Terms

Marine operations, model predictive control, hydrodynamic modelling, wave prediction, dynamic positioning.

*Center for Autonomous Marine Operations and Systems, Department of Engineering Cybernetics, Norwegian University of Science and Technology, Trondheim, Norway.

**Kongsberg Maritime, Ålesund, Norway.

Manuscript received November 26, 2023; revised —

I. Introduction

Dynamic positioning (DP) is defined as a vessel's capability to automatically maintain its position and heading exclusively by the means of its thrusters [1], [2]. DP systems on conventional vessels are designed to compensate primarily for the slowly time-varying forces due to wind, ocean current and second-order wave drift. They employ wave frequency filtering of the position and velocity measurements so that the DP feedback control does not compensate for first-order wave motions, [3], [4]. The main reasons for this is that it may not be necessary for many operations and that many thrusters do not have a sufficiently fast dynamical response. It would also increase fuel consumption, and fast power load variations cause excessive wear of the machinery system and the thrusters themselves.

Conventional DP control algorithms are commonly implemented as two modules. First there is a high-level control algorithm which determines the generalised force required to control position and heading. This control design problem has weak nonlinearities and the axes are decoupled, so three PID controllers is a state-of-the-art solution, [2]. The second module is a thrust allocation algorithm, where this generalised force vector is transformed into force commands to each individual thruster. The thruster dynamics are usually not explicitly considered in the high-level motion control algorithm. Effects such as saturation, asymmetric propellers and rate limitations are therefore not explicitly accounted for when the controller determines the required generalised force. If the thrusters cannot instantly produce the required force on the vessel, the controller will behave sub-optimally. Most commonly thrust allocation is done by solving an optimisation problem, [5]. Optimisation-based thrust allocation algorithms can incorporate physical and operational constraints, ie. saturation, rate limitations and forbidden sectors, in the optimisation problem. This can be handled sub-optimally using thrust allocation and power management functionality that can mitigate fast load variations and prevent blackout using thrust limitation, reduction, biasing and modulation, [6], [7], [8].

A more recent development in the field of dynamic positioning is the use of model predictive control (MPC), which relies on solving an optimal control problem using online numerical optimization. An early application of MPC for dynamic positioning was presented in [9], where a MPC was used for dynamic positioning of a semi-submersible platform in calm conditions. In [10] a tube-based MPC controller was implemented and tested with varying disturbances. In [11] the high level control and thrust allocation was integrated into a single MPC that was shown to achieve improved performance in highly dynamic conditions where the thruster dynamics and constraints makes the integrated approach favourable. This results in the constraints being included in the motion control problem and the control force can therefore be made optimal with respect to the constraints.

Our research is motivated by emerging smaller vessel concepts. One example is offshore service vessels for inspection, maintenance and repair (IMR). Such vessels typically support remotely operated vehicle (ROV) operations where the surface vessel's DP capabilities are crucial in order to maintain the vessel in close proximity to the ROV. Some new vessel concepts are designed to be unmanned and much smaller in size than conventional IMR vessels. Then the first order wave-driven oscillatory motion may be large. This motivates the use of DP control to actively compensate also for first order wave driven horizontal motions in order to increase operability during certain operations such as launch and recovery of the ROV through the wave zone. Such operations take short periods of time such that wear on thrusters and machinery is not a concern. This paper's objective is to study DP systems that can compensate for first-order wave-driven horizontal vessel motions.

This is a problem that has not received much attention in the literature. The principal approach that has been proposed in the literature to reduce rapidly varying environmental forces is the use of acceleration feedback [12], [13]. The idea is that conventional DP based on position and velocity feedback will experience a delay in its response, since it takes some time before a force imbalance leads to a position or velocity error that the feedback controller compensates for. Acceleration feedback provides a more direct measurement of the force imbalance and can detect the effects of wave forces immediately. Acceleration feedback may be effective, but is limited by thruster dynamics that will lead to a lag in the acceleration feedback that may significantly deteriorate the performance. However, the mentioned controllers are not designed to explicitly account for limitations due to thruster dynamics, saturation, and limited availability of electrical power to the thrusters from diesel-electric power systems. Moreover, they do not exploit feed-forward control from wave disturbance predictions.

Wave prediction methods can be separated into two categories. Model-based methods, such as SWAN [14], makes models that mimic the physical world and makes predictions based on these models. Machine learning methods, [15], [16], aims to find patterns in data to fit a model and are shown to provide more accurate predictions on horizons shorter than 5 hours [17]. Wave predictions over time horizons as long as hours aims to predict the statistical characteristics of waves, such as wave height and the wave period. While this is sufficient to describe the general behaviour of the waves, it does not give an accurate prediction of individual waves. The phase angle of the waves are often considered to be randomly distributed as the effect of varying phase will cancel out over large time horizons. To accurately predict individual waves for wave-compensating control, a much shorter time scale is needed. An accurate short-term wave prediction with a horizon of less than 20 seconds can be achieved by using an auto-regressive model trained on a separate data set [18]. Another approach is to use a model consisting of a fixed number of harmonic component and use a predefined set of frequencies [19]. That way the amplitudes and phases can be determined by a linear least-squares problem. This eliminates the need of a separate data-set as the model parameters can be determined online.

In this paper we propose an integrated dynamic positioning control design that is intended to compensate actively for first-order wave-induced motions. The novel idea is to predict the wave-induced motion for a short period of time based on a novel adaptive estimator for the wave-induced motions driven by measurements of vessel velocity. These real-time predictions are used in an MPC to predict the short-term wave-induced motion disturbances, and optimally compensate for them by considering dynamic models and limitations in the thruster system.

This paper is organised as follows: In section II the mathematical model used for prediction in the controller is presented. Section III presents the prediction algorithm used to predict the wave-induced motion on the vessel before the MPC problem formulation is presented in Section IV. The proposed controller is tested in simulations and the results are presented in Section V.

II. VESSELS MODELLING

This section presents the model used in the controller for predicting the future behaviour of the system. It is based on a horizontal-plane model from [2].

A. Kinematics

The vessel considered here is assumed to operate at a limited geographical area. The vessel position can then be described relative to a North-East-Down (NED) reference frame fixed to the ocean surface with its x-axis pointing North, y-axis pointing East and z-axis pointing downwards. The origin of the reference frame is the DP setpoint. The vessel position and heading in the reference frame is given by $\eta = [x, y, \psi]^T \in \mathbb{R}^3$, where x is the North-position, y is the East-position and ψ is the heading of the vessel relative to North in the horizontal plane.

The velocity of the vessel is described relative to a separate body-fixed reference frame. This reference frame has its origin at the centre of the ship. The x-axis is pointing towards the bow of the ship, the y-axis is pointing directly towards starboard and the z-axis is pointing directly downwards. The generalised velocity of the vessel in the body-fixed reference frame is given by $\nu = [u, v, r]^T \in \mathbb{R}^3$, where u is the velocity along the x-axis, v is the velocity along the y-axis and r is the angular velocity around the z-axis. The relationship between the velocity in the body-fixed reference frame and the NED reference frame is given by

$$\dot{\eta} = \begin{bmatrix} \cos(\psi) & -\sin(\psi) & 0 \\ \sin(\psi) & \cos(\psi) & 0 \\ 0 & 0 & 1 \end{bmatrix} \nu \tag{1}$$

or on vector form

$$\dot{\eta} = \mathbf{R}(\psi)\nu. \tag{2}$$

B. Vessel Dynamics

The forces and torques (called generalised forces taken together) from several physical sources act on the vessel. Most notably are environmental forces and hydrodynamic forces. Assuming constant and irrotational ocean currents, the generalised velocities in 6 degree of freedom, here denoted ν^* as a result of a sum of external forces can be written

$$(\mathbf{M}_{RB}+\mathbf{M}_A(\infty))\dot{\nu}_r^*+(\mathbf{C}_{RB}(\nu_r^*)+\mathbf{C}_A(\nu_r^*))\nu_r^*+(\mathbf{B}(\infty)+\mathbf{B}_V(\infty))\nu_r^*+\mu_r^*+\mathbf{G}\eta^* = \tau_{wind}+\tau_{wave}+\tau \tag{3}$$

where $\mathbf{M}_{RB} \in \mathbb{R}^{6\times 6}$ is the rigid body inertia matrix, $\mathbf{M}_\infty \in \mathbb{R}^{6\times 6}$ is the added mass matrix at infinite frequency, $\mathbf{C}_{RB}(\nu_r^*) \in \mathbb{R}^{6\times 6}$ and $\mathbf{C}_A(\nu_r^*) \in \mathbb{R}^{6\times 6}$ are the Coriolis and centripetal force matrix due to inertia and added mass, $\mathbf{B}(\infty) \in \mathbb{R}^{6\times 6}$ and $\mathbf{B}_V(\infty) \in \mathbb{R}^{6\times 6}$ are the potential and viscous damping matrix at infinite frequency, $\mu_r^* \in \mathbb{R}^6$ is the fluid memory effects represented with a set of impulse functions, $\mathbf{G} \in \mathbb{R}^{6\times 6}$ is the restoring force matrix and $\tau \in \mathbb{R}^6$ are the wind, waves and control forces. This model is a nonlinear time-domain model incorporating frequency dependent hydrodynamic forces [2].

For the controller model we want to simplify the full 6 degree of freedom model shown in Equation (3). A vessel operating in DP is assumed to have a low velocity and low rate of change in yaw, therefore the Coriolis and centripetal effects can be neglected [20]. When reducing the model to the 3 degrees of freedom surge, sway and yaw, the restoring forces will disappear.

Finally we apply the assumption that when applying the feedback control system to stabilize the motions in surge, sway and yaw the natural frequencies will be close to zero [2]. We can therefore replace the frequency dependent added mass and damping matrices $\mathbf{M}_A(\omega)$, $\mathbf{B}(\omega)$ and $\mathbf{B}_V(\omega)$ with the constant matrices $\mathbf{M}_A(0)$, $\mathbf{B}(0)$ and $\mathbf{B}_V(0)$. This will remove the fluid memory effects, μ_r and we are left with the linear model

$$\mathbf{M}\dot{\nu}_r + \mathbf{D}\nu_r = \tau_{wind} + \tau_{wave} + \tau, \tag{4}$$

where $\mathbf{M} = \mathbf{M}_{RB} + \mathbf{M}_A(0)$ and $\mathbf{D} = \mathbf{B}(0) + \mathbf{B}_V(0)$

C. Thruster Modelling

An azimuth thruster located at $r_i = [l_{xi}, l_{yi}, l_{zi}]^T$ in the body-fixed reference frame generating a specific force f_i in the direction α_i will produce a generalized force according to

$$\tau = \begin{bmatrix} \cos\alpha_i \\ \sin\alpha_i \\ l_{xi}\sin\alpha_i - l_{yi}\cos\alpha_i \end{bmatrix} T_i. \tag{5}$$

The number of thrusters is N_{th} such that the total generalised force $\tau = \sum_{i=1}^{N_{th}}$ acting on the vessel is given by

$$\tau = \mathbf{B}(\alpha)\mathbf{T} \tag{6}$$

where $\mathbf{B}(\alpha) \in \mathbb{R}^{3\times N_{th}}$ is the thruster configuration matrix and $\mathbf{T} = [T_1, ..., T_{N_{th}}]^T \in \mathbb{R}^{N_{th}}$ is the thrust produced by each individual thruster.

A thruster can be modelled as an electrical motor driving a shaft with a propeller. The angular acceleration of the shaft $\dot{\omega}_m$ is determined by the sum of torques acting on it. Assuming the shaft is rigid, this gives

$$I_{RB}\dot{\omega}_m = Q_m - Q_L. \tag{7}$$

where $I_{RB} \in \mathbb{R}$ is the inertia of the shaft, $Q_m \in \mathbb{R}$ is the torque from the electrical motor and $Q_L \in \mathbb{R}$ is the load torque.

An object submerged in water will experience an additional force or torque due to the requirement of accelerating the surrounding water when it moves. For the rotating shaft considered here this will result in an additional torque proportional to the angular acceleration, called *hydrodynamic added inertia* leading to a total inertia I.

The friction torque can be modelled as a combination of Coulomb friction and linear viscous friction. The Coulomb friction is a constant torque for all angular velocities, while the linear viscous friction torque increases linearly with angular velocity. The total friction torque can be written

$$Q_f = k_1 \text{sign}(\omega_m) + k_2 \omega_m \tag{8}$$

where k_1 and k_2 are friction coefficients. The function sign(ω_m) is not continuous at $\omega_m = 0$. To get a continuous model suited for gradient-based optimization, sign(ω_m) can be approximated by a continuous function

$$\text{sign}(\omega_m) \approx \frac{2}{\pi} \arctan\left(\frac{\omega_m}{\epsilon}\right) \tag{9}$$

where $\epsilon \in \mathbb{R}$ is a small positive number.

The torque exerted on the shaft by the propeller is highly nonlinear, and depends on factors such as propeller shape, relative velocity of the water passing by the propeller and pressure differences in the wake created by the hull. To simplify this dynamic relationship the open water characteristics of the propeller can be used to find an expression for the torque and thrust produced by the propeller. When using open water characteristics, interactions between the propeller and the hull are neglected. The open water characteristics of the propeller can be expressed as the thrust and torque coefficients [21]

$$K_T = T \frac{4\pi^2}{\rho \omega_m |\omega_m| D^4} \tag{10}$$

$$K_Q = Q \frac{4\pi^2}{\rho \omega_m |\omega_m| D^5} \tag{11}$$

where T is the thrust, ρ is the water density, D is the diameter of the propeller and Q is the torque of the propeller.

The propeller is assumed to be asymmetric. An asymmetric propeller is less effective when operating in reverse, thus it will have different thrust and torque coefficients in each direction. The torque of the propeller can be written

$$Q_p = G_p \omega_m |\omega_m| \tag{12}$$

where

$$G_p = \begin{cases} K_{Q0} \frac{\rho D^5}{4\pi^2} & \omega_m \geq 0 \\ K_{Qr} \frac{\rho D^5}{4\pi^2} & \omega_m < 0 \end{cases}. \tag{13}$$

The coefficients K_{Q0} and K_{Qr} are the torque coefficients for the forward direction and reverse direction respectively.

The thrust coefficient can be used to find an expression for the thrust generated by each thruster as a function of the angular velocity. This gives

$$T = K_p \omega_m |\omega_m| \tag{14}$$

where

$$K_p = \begin{cases} K_{T0} \frac{\rho D^4}{4\pi^2} & \omega_m \geq 0 \\ K_{Tr} \frac{\rho D^4}{4\pi^2} & \omega_m < 0 \end{cases} \tag{15}$$

Here K_{T0} and K_{Tr} are the thrust coefficients for the forward direction and reverse direction respectively.

The resulting thruster model is given by

$$I\dot{\omega}_m = Q_m - G_p \omega_m |\omega_m| - k_1 \frac{2}{\pi} \arctan\left(\frac{\omega_m}{\epsilon}\right) - k_2 \omega_m. \tag{16}$$

For a vessel with N_{th} thrusters, the thruster dynamics can be written om matrix form

$$\mathbf{I}\dot{\omega}_m = \mathbf{Q} - \mathbf{Q}_p - \mathbf{Q}_f \tag{17}$$

where ω_m is a vector with the thruster angular velocities, $\mathbf{I} = \text{diag}(I_1, I_2, ..., I_{N_{th}})$ is total inertia, $\mathbf{Q} = [Q_1, Q_2, ..., Q_{N_{th}}]^T$ is the torque exerted on the shaft by the electrical motor, $\mathbf{Q}_p = [Q_{p1}, Q_{p2}, ..., Q_{pN_{th}}]^T$ is the propeller torque and $\mathbf{Q}_f = [Q_{f1}, Q_{f2}, ..., Q_{fN_{th}}]^T$ is the friction torque. The thrust produced by the N_{th} thrusters is

$$\mathbf{T} = \mathbf{H}(\omega_m) \tag{18}$$

where $\mathbf{H}(\omega_m) = [K_{p1}\omega_{m1}|\omega_{m1}|, ..., K_{pN_{th}}\omega_{mN_{th}}|\omega_{mN_{th}}|]^T$.

III. Environmental Forces and Short-Term Wave Motion Prediction

For the controller to be able to predict future disturbances due to environmental forces, a separate wave motion prediction algorithm is necessary. By using linear wave theory, a model of the wave-induced velocity due to regular waves can be derived. An advantage of linear wave theory is that a description of an irregular sea can be obtained by superimposing a number of regular waves, thus extending the model to account for irregular waves is straight-forward. Waves can be considered to consist of a high-frequency oscillating part and a slowly varying part (first- and second-order waves, respectively). The wave model presented here will be capable of predicting both high-frequency oscillating wave forces and slowly varying wave forces. Forces due to ocean currents and winds will be considered to be slowly varying forces too, such that they can be lumped together with second-order wave forces in the model.

The model parameters can be estimated by minimising the squared error of the wave model predictions and a set of measurements, as shown in Section III-E. This can be done online, making the prediction adaptive to changes in the sea environment. This is contrary to most wave prediction algorithms, which estimates the model parameters offline. The approach presented here is chosen for its generality. It requires few parameters to be set and offers good flexibility. The only requirement is knowledge about the vessel model and measurements of its velocity. The algorithm is able to achieve sufficiently accurate predictions of induced forces due to environmental conditions for 10 to 15 seconds [22].

A. *Wave Model*

In linear wave theory an irregular wave can be approximated as a sum of regular waves with different frequencies, phase and amplitudes [23]. The wave height of a short-crested wave is given by

$$\zeta(t) = \sum_{i=1}^{N_h} \sum_{m=1}^{M} A(\omega_i, \theta_m) \sin\left(\omega_i t - k_i x \cos\theta_m - k_i y \sin\theta_m + \epsilon_i\right) \tag{19}$$

where N_h is the number regular wave components, M is the number of directions, $A(\omega, \theta)$ is the amplitude as a function of the wave frequency and wave direction, ω is the wave frequency, k is the wave number, (x, y) denotes the position in the horizontal plane, θ is the wave direction and ϵ is a random phase angle. If we assume the wave height is considered only at a fixed geographical location, that is (x, y) is constant, the wave height simplifies to

$$\zeta(t) = \sum_{i=1}^{N_h} A_i \sin\left(\omega_i t + \epsilon_i\right). \tag{20}$$

This makes the model only valid for applications with constant or slowly varying position. High frequency components tend to become insignificant [24], thus realistic waves can be represented with a relatively small N_h.

The wave height model presented in Equation (20) assume the waves can be modelled as a stationary random process. This means that for each frequency in Equation (20), the corresponding amplitude and phase will be constant. This is a good assumption over a short period of time, but in reality the model parameters will be varying with time due to nonlinear wave interactions, tides and weather changes.

B. Wave induced motion model

With a linear description of the waves, both the velocity and acceleration of the waves are linearly proportional to the height of the wave $\zeta(t)$. This also implies that the forces acting on the vessel by the waves are linearly proportional to the wave height. Since the vessel dynamics are linear there is a linear relationship between the velocity of the vessel and the forces acting on it. Assuming for the moment that the wave-induced forces are the only forces acting on the vessel, the wave-induced velocity can be written

$$\nu_w(t) = \sum_{i=1}^{N_h} \mathbf{A}_i \left|\mathbf{G}(j\omega_i)\right| \sin\left(\omega_i t + \angle\mathbf{G}(j\omega_i) + \epsilon_i\right) \tag{21}$$

where $\nu_w \in \mathbb{R}^3$ is the component of the 3 DOF generalised velocity of the vessel that is the result of the waves, $\mathbf{G} \in \mathbb{R}^3$ is a vector of transfer functions relating the wave height to the induced velocity and $\mathbf{A}_i \in \mathbb{R}^3$, $\omega_i \in \mathbb{R}^3$ and $\epsilon_i \in \mathbb{R}^3$ are the model parameters. The parameters of the model can be found by fitting it to data of the velocity, which is assumed to be measured at all times. The velocity model is a smooth function and by taking the time derivative, a model for acceleration can be found to be

$$\dot{\nu}_w(t) = \sum_{i=1}^{N_h} \mathbf{A}_i\omega_i \left|\mathbf{G}(j\omega_i)\right| \cos\left(\omega_i t + \angle\mathbf{G}(j\omega_i) + \epsilon_i\right). \tag{22}$$

The wave-induced force in surge, sway and yaw can then be obtained by using the vessel dynamics

$$\tau_{wave}(t) = \mathbf{M}\dot{\nu}_w(t) + \mathbf{D}\nu_w(t), \tag{23}$$

where $\mathbf{M}$ and $\mathbf{D}$ are given in Equation (4).

C. Ocean Current, Wind and Second-Order Wave Forces

Forces due to steady-state ocean currents, wind and second-order wave-induced forces are not included in the model above. For a short period of time we can assume the wind, second-order waves and ocean current velocities are constant. The constant environmental velocities can then be assumed to give a constant shift in velocities. Augmenting the model to account for this gives

$$\nu_{env}(t) = \mathbf{C} + \sum_{i=1}^{N_h} \mathbf{A}'_i \sin\left(\omega_i t + \phi_i\right) \tag{24}$$

where $\mathbf{C} \in \mathbb{R}^3$ is a vector of constants. We have collected all constant terms such that for a given frequency ω_i we have $\mathbf{A}_i' = \mathbf{A}_i \left|\mathbf{G}(j\omega_i)\right|$ and $\phi_i = \angle\mathbf{G}(j\omega_i) + \epsilon_i$ that describes the vessel's wave-induced motion. Note that $\nu_{env}(t)$ now models the induced velocity due to all environmental forces, not only waves. Equation (23) can then be generalized to

$$\tau_{env}(t) = \mathbf{M}\dot{\nu}_{env}(t) + \mathbf{D}\nu_{env}(t). \tag{25}$$

Wind forces might have components that are faster due to wind gusts and turbulence. These forces might also be compensated for by the DP just as first order wave forces, and from a practical point of view we can consider these dynamic wind effects within the same mathematical framework and consider them part of τ_{env} and ν_{env}.

D. Wave Force Prediction Algorithm

A prediction algorithm can now be made on the basis of the model derived above. Discretizing the general model of induced velocity given in Equation (24) gives

$$\nu_{env,k} = \mathbf{C} + \sum_{i=1}^{N_h} \mathbf{A}_i' \sin\left(\omega_i \Delta T_{wf} k + \phi_i\right) \tag{26}$$

where ΔT is the sampling interval and k is an integer representing the current time instance such that $t = \Delta T k$. The model parameters are estimated with respect to a finite set of previous measurements of the generalised velocity $\nu(t)$. Given the measurement $\mathbf{y}_m = (u_m, v_m, r_m) \in \mathbb{R}^3$ of $\nu(t)$ and a backwards estimation window of N_b samples, the data used to estimate the model parameters are contained within the set

$$\Omega = \{\mathbf{y}_m \in \mathbb{R}^3 \mid m \in \mathbb{Z}, k - N_b \leq m < k\} \tag{27}$$

The time window of velocity measurements within Ω is then $T_b = N_b \Delta T$. We let the model of the velocity with parameters estimate with respect to the measurements in Ω be denoted $\hat{\nu}_{env,k}$. Furthermore, a prediction l steps into the future from time instance k based on the estimated model $\hat{\nu}_{env,k}$ can be denoted $\hat{\nu}_{env,k+l|k}$. This gives the following prediction algorithm

$$\hat{\nu}_{env,k+l|k} = \mathbf{C} + \sum_{i=1}^{N_h} \mathbf{A}_i' \sin\left(\omega_i \Delta T(k+l) + \phi_i\right). \tag{28}$$

The corresponding prediction of acceleration is given by

$$\hat{\dot{\nu}}_{env,k+l|k} = \sum_{i=1}^{N_h} \mathbf{A}_i' \omega_i \cos\left(\omega_i \Delta T(k+l) + \phi_i\right). \tag{29}$$

With a prediction of both the velocity and acceleration, the induced forces due to environmental disturbances in the horizontal plane can be predicted with

$$\hat{\tau}_{env,k+l|k} = \mathbf{M}\hat{\dot{\nu}}_{env,k+l|k} + \mathbf{D}\hat{\nu}_{env,k+l|k}. \tag{30}$$

E. Estimation of Model Parameters

The model parameters can be found by minimising the least-squares criteria between the model and the measurements in Ω. Since the vessel model is decoupled in surge, sway and yaw, a separate, but identical, optimisation problem can be solved for each degree of freedom. Only the surge velocity will be considered here. The model for the induced velocity due to environmental forces in surge is

$$\hat{u}_{env,k} = C + \sum_{i=1}^{N_h} A'_i \sin(\omega_i \Delta T k + \phi_i). \tag{31}$$

Minimising the sum of the squared error gives the following moving-window optimisation problem

$$\underset{\Theta}{\text{minimise}} \quad \frac{1}{2} \sum_{m=k-N_b}^{k-1} (\hat{u}_{env,m}(\Theta) - u_m)^2 \tag{32}$$

where $\Theta = [C, A'_1, ..., A'_{N_h}, \omega_1, ..., \omega_{N_h}, \phi_1, ..., \phi_{N_h}]^T \in \mathbb{R}^{3 \times N_h + 1}$ is a vector of the model parameters to be estimated and u_m is the measurement of the surge velocity. The velocity model (31) is nonlinear in both phase and frequency, which makes the optimisation problem nonlinear.

The optimisation problem can be solved as it is stated now, but the rate of convergence can be improved by introducing constraints. The constraints can be determined on the basis of physical properties of the wave, ie. unrealistically high amplitudes can be excluded:

$$0 \leq A_i \leq A_{max}, \qquad i \in [1, N_h] \tag{33}$$

$$-\pi \leq \phi_i \leq \pi, \qquad i \in [1, N_h] \tag{34}$$

$$\omega_{min} \leq \omega_i \leq \omega_{max}, \qquad i \in [1, N_h] \tag{35}$$

The optimization problem is in this paper solved at each sampling instant using a nonlinear least-squares numerical optimization algorithm, but we note that it can alternatively be solved asymptotically with lower computational complexity using a recursive nonlinear least-squares algorithm, [25].

F. Dependency Between Wave Prediction and Thrusters

When deriving the model of induced velocity due to environmental forces, it was assumed that the only forces acting on the vessel was the environmental forces. This assumption does not hold true in DP, as the thrusters will act on the vessel with a force τ. To relax the assumption of no thruster forces, the effect of the thrusters on the vessel must be removed from the prediction algorithm.

The vessel model is linear under the assumption of low velocity, thus using the principle of superposition the velocity of the ship can be split into two components: the velocity induced by the thrusters and the velocity induced by the environmental forces wind, waves and ocean current. As shown in the previous section the vessel velocity is modelled

$$\mathbf{M}\dot{\nu} + \mathbf{D}\nu = \tau + \tau_{env} \tag{36}$$

The total velocity ν can be separated into the two components $\nu = \nu_t + \nu_{env}$ where ν_t is the velocity of the vessel due to thruster-induced forces and ν_{env} is the velocity due to environmental forces acting on the vessel. This gives

$$\mathbf{M}\dot{\nu}_t + \mathbf{D}\nu_t = \tau \tag{37a}$$

$$\mathbf{M}\dot{\nu}_{env} + \mathbf{D}\nu_{env} = \tau_{env}. \tag{37b}$$

The generalised force τ is modelled with the thrust allocation matrix given in Equation (6) and the thruster model given in Equation (17) and (18). The generalised forces τ due to the thrusters can therefore be considered known at all times. The thruster-induced velocity ν_t can then be found by solving the differential equation (37a). As ν is measured by the sensors of the vessel, ν_{env} is given by

$$\nu_{env} = \nu - \nu_t \tag{38}$$

This isolates the velocity component due to environmental forces and the model parameters can be estimated based on this velocity. This will cancel out the effect of the thrusters when the model parameters are estimated.

IV. MPC Formulation

The continuous-time MPC problem formulation is presented here.

$$J^* = \min_{Q,\dot{\alpha}} \quad \int_0^T ||\eta - \eta_{ref}||^2_{Q_\eta} + ||\nu||^2_{Q_\nu} + ||Q||^2_{R_Q} + ||\dot{\alpha}||^2_{R_{\dot{\alpha}}}\, dt \tag{39a}$$

$$\text{s.t.} \quad \text{Initial conditions on } \eta, \nu, \omega_m, \alpha, Q \tag{39b}$$

$$\dot{\eta} = \mathbf{R}(\psi)\nu \tag{39c}$$

$$\mathbf{M}\dot{\nu} + \mathbf{D}\nu = \tau + \tau_{env} \tag{39d}$$

$$\mathbf{I}\dot{\omega}_m = \mathbf{Q} - \mathbf{Q}_p - \mathbf{Q}_f \tag{39e}$$

$$\tau = \mathbf{B}(\alpha)\mathbf{T} \tag{39f}$$

$$\mathbf{T} = \mathbf{H}(\omega_m) \tag{39g}$$

$$Q_{min} \leq Q_i \leq Q_{max}, \quad i \in \{1, N_{th}\} \tag{39h}$$

$$\alpha_{min} \leq \alpha_i \leq \alpha_{max}, \quad i \in \{1, N_{th}\} \tag{39i}$$

$$\left|\dot{Q}_i\right| \leq \dot{Q}_{max}, \quad i \in \{1, N_{th}\} \tag{39j}$$

$$|\dot{\alpha}_i| \leq \dot{\alpha}_{max}, \quad i \in \{1, N_{th}\} \tag{39k}$$

where η_{ref} is the DP's reference point for position and heading.

The objective function (39a) consists of quadratic penalty terms on deviations in position, velocity and the use of the control variables. Minimising the position error will control the vessel towards the setpoint while minimising the velocity error will give a damping effect. Penalising the control variables will avoid unnecessary use of the thrusters. Non-quadratic penalty terms for minimising the power consumption can be added, but this is not considered here.

The constraints in (39b) represents the initial conditions given by the current state and control variables.

The control variables control the torque of each thruster. For generality, it is assumed that azimuth thrusters are used, so direction of the thruster in the horizontal plane may also be controlled. The thrusters will have physical limitations and not all possible control trajectories are feasible for the dynamic system. The thruster can be limited to rotate in a given sector. This can be of both physical and operational considerations. A constraint on the angle of rotation is included in (39i). If the thruster is not rotating, ie. a tunnel thruster, the direction will be fixed. The rate at which a rotating thruster can rotate about it own axis will be limited, thus a constraint on the rate of change of the thruster direction is necessary. This is included in (39k).

The thrusters will also be limited by how much torque can be produced by the electrical motor. This will limit the angular velocity of the propeller and thereby the thrust produced. This limitation is included in constraint (39h). Thrusters are typically not symmetric, that is they are less effective when operating in reverse. This is included in the thruster model in the controller and therefore accounted for. An asymmetric propeller results in different torque limitations depending on the direction of the propeller. This must be reflected in constraint (39h).

The thrusters are often limited in how fast the torque can increase. A fast increase in torque will result in a large variation in the power demand, potentially resulting in a blackout. Rate limitations on the thruster torque are included to prevent this. This is included in constraint (39j).

The constraints (39c) and (39d) are the kinematics and dynamics of the vessel. The constraint (39e) represents the dynamics of N_{th} thrusters. The thrust configuration matrix in (39f) shows the relationship between the generalised force vector on the vessel and the individual thruster forces while the constraint represented in (39g) gives the specific force of each thruster as a function of the angular velocity of its propeller.

The vector τ_{env} in (39d) contains the generalised environmental forces acting on the vessel. The value of the environmental forces at the current time can be obtained with various sensors, but the future value cannot be known. This is one of the major limitations with applications of predictive control in dynamic and stochastic environments. Traditionally the environmental disturbances are estimated at the current time and considered to be constant over the prediction horizon. Here we will considered a more dynamic approach where a prediction of the environmental disturbances is obtained using the prediction algorithm described in Section III.

The prediction algorithm is included in the controller by replacing τ_{env} with $\hat{\tau}_{env,k+l|k}$ where

$$\hat{\tau}_{env,k+l|k} = \mathbf{M}\hat{\dot{\nu}}_{env,k+l|k} + \mathbf{D}\hat{\nu}_{env,k+l|k} \tag{40}$$

$$\hat{\nu}_{env,k+l|k} = \mathbf{C} + \sum_{i=1}^{N_h} \mathbf{A}'_i \sin\left(\omega_i \Delta T_{wf}(k+l) + \phi_i\right) \tag{41}$$

$$\hat{\dot{\nu}}_{env,k+l|k} = \sum_{i=1}^{N_h} \mathbf{A}'_i \omega_i \cos\left(\omega_i \Delta T_{wf}(k+l) + \phi_i\right) \tag{42}$$

where the wave-induced motion parameters Θ are estimated at each sampling instant as described in Section III-E. The constant term in the model will predict constant and slowly varying disturbances. This has a similar effect as integral action in a conventional PID controller. It is therefore not necessary to include dedicated states in the controller to get integral effect.

The continuous problem formulation given in (39) must be discretised in order to be implemented by a digital computer. A direct approach is used where the continuous problem is approximated by discretising it and then solved as a nonlinear optimisation problem. The fourth order Runge-Kutta numerical integration method is then used to do a forward simulation of the dynamic system, transforming the dynamics to a set of equality constraints. This approach is called direct multiple shooting, where both the state variables and the control variables are variables to be optimised. That means the controller will give out both optimal control trajectories and optimal state trajectories. Both the state trajectories and control trajectories can then be used as an initial guess of the variables in the next iteration of the controller.

V. Simulation Result

Simulations are run to evaluate the performance of the proposed MPC. The proposed MPC with wave prediction, referred to as MPC-WP, is compared to a MPC baseline controller without wave prediction, similar to the one presented in [11]. The vessel controlled is 24m long and has a mass of 1.53×10^5kg. The vessel is equipped with two azimuth thrusters, based on [26], placed along the centre line fore and aft. The thrusters are rated at 160 kW and can produce a thrust of 37 kN. The maximum azimuth turning rate is set to $30°/s$ and the thruster is limited to rotate in a sector of $\pm 90°$. The thruster torque, which is controlled by the MPC, has a ramp-up time of 2 seconds. The simulator is implemented in Matlab/Simulink using the Marine Systems Simulator (MSS) toolbox [27]. The dynamics of the vessel are simulated using the nonlinear dynamics presented in Equation (3), where the frequency dependent added mass and damping are computed using WAMIT [28]. The controllers are implemented using CasADi with the solver IPOPT [29], [30]. The waves are generated using the JONSWAP wave spectrum with the peak-shaping parameter $\gamma = 3.3$ and 10 directional components in all cases. The prediction horizon of the controllers are set to 15 seconds and the discretization interval is set to 0.25 seconds. When wave prediction is used, the wave model is set up with 3 harmonic components and the length of the moving window is set to 15 seconds. Initially the performance of the controllers is validated by running three different scenarios with increasingly challenging conditions. To evaluate the contribution of the wave prediction integrated in the controller over time, a Monte

Carlo (MC) simulation is run for three different sea states and the performance evaluated by computing the position mean error

$$ME = \frac{1}{M}\sum_{i=1}^{M}(x_{pos,i} - x_{ref}), \tag{43}$$

the root mean square error (RMSE) of the positioning in the horizontal plane

$$RMSE = \sqrt{\frac{1}{M}\sum_{i=1}^{M}(x_{pos,i} - x_{ref})^2}, \tag{44}$$

the maximum absolute error (MAE) in the horizontal plane

$$MAE = \max\left\{|x_{pos,i} - x_{ref}|\right\}, \quad i \in [1, M], \tag{45}$$

and the normalized net force deviation

$$NNFD = \sqrt{\frac{\sum_{i=1}^{M}(\tau_{waves,i} + \tau_{control,i})^2}{\sum_{i=1}^{M}\tau_{waves,i}^2}}. \tag{46}$$

A. Simulation Scenarios

Initially, three simulation scenarios are run in order to validate the performance of the controllers. For the two first scenarios no waves are present, thus the two controllers are identical as the wave prediction will not be active. A prediction of the constant disturbances is included in order to provide integral action for the controllers. The purpose of these two scenarios is to validate and illustrate the basic control performance without waves. For the third scenario, waves are included and thus the two controllers differ. For all scenarios the thrusters are initialized in it default position, pointing towards the stern of the vessel, and with zero angular velocity of the propellers. The reference position and heading are set to zero. Each of the three scenarios are described in Table I.

1) First scenario: The first simulations show the controller correcting for a starting position away from the reference position. The vessel is successfully controlled to its reference within about 40 seconds. A small weight is placed on the use of thrust to ensure the thrusters are turned of as the vessel reaches the reference point. As there is no cost on the direction of the azimuth thrusters, only on the rate of change, the thrusters will not rotate back to its default position.

Scenario	Start position	Current (Speed / Direction)	Waves (Significant wave height / Peak period / Direction)
1	$[2\ 0\ 20°]^T$	0 m/s / 0°	0m / 0s / 0°
2	$[2\ 0\ 20°]^T$	0.3 m/s / 15°	0m / 0s / 0°
3	$[2\ 0\ 20°]^T$	0.3 m/s / 15°	5m / 12s / 0°

TABLE I

SIMULATION SCENARIOS

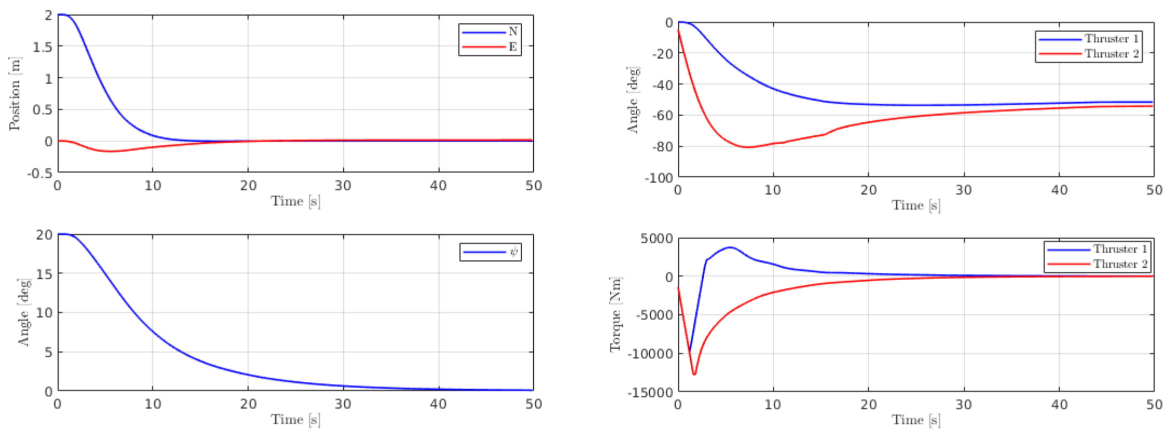

(a) Vessel position

(b) Thruster angle and torque

Fig. 1. Vessel position and thruster controls for the first scenario.

2) Second scenario: The second simulations show the same scenario as presented before with the only difference of added current. The controller is successful in reaching the reference within about 50 seconds. The current introduces a constant disturbance and the thrusters converge to a constant angular velocity and direction in order to counteract this. The integral action in the controllers is successful in compensating for the constant disturbance as the position converge to its reference.

3) Third scenario: In the third scenario waves are included as well, thus the controllers will differ. Figure 3 show the vessel position and controls for the two controllers. Both controllers are successful in counteracting the current and maintain its mean position at the reference point, however, they differ significantly in their ability to counteract first order waves. The MPC with wave prediction is far better at removing wave induced oscillations in the position and heading. Figure 4 shows the force exerted on the vessel by the waves and thrusters as well as the sum of these two forces for both controllers. Initially they perform identically as the wave prediction

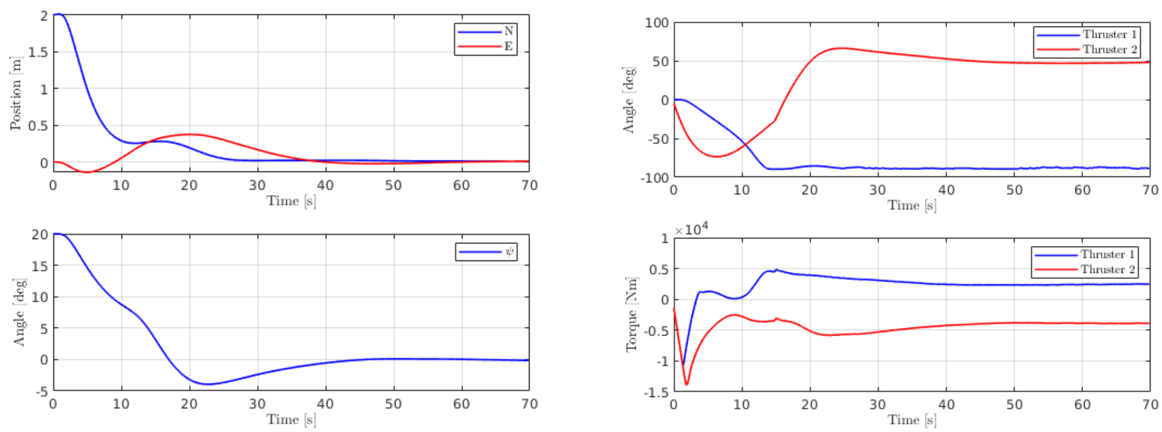

(a) Vessel position

(b) Thruster angle and torque

Fig. 2. Vessel position and thruster controls for the second scenario.

need 15 seconds of recorded data to start its prediction. After about 20 seconds, Figure 4 shows that the force produced by the thruster for the MPC with wave prediction reaches a similar amplitude as the wave force with a phase offset off $180°$, canceling out most of the wave induced forces as shown by the net force. This does not happen for the baseline controller. In fact, the baseline controller amplifies the wave induced force and end up with a larger wave induced position error. It shows that wave compensation without an accurate wave prediction can lead to worse performance.

The effect of the thruster constraints appears to clearly effect the baseline controllers ability to control the position. The rate of change of torque for the baseline controller is saturated through the entire scenario, as seen in Figure 3d, while for the MPC with wave prediction the rate of change is mostly saturated only at the beginning before the wave prediction is active, seen in Figure 3b. As a result, the MPC with wave prediction have a energy usage of only 73% of the energy the MPC baseline controller uses while still achieving a better position accuracy.

How the controller makes use of the wave prediction is demonstrated in Figure 5, showing the optimal north-position trajectory and the optimal torque control trajectory for one thruster as computed by the MPC at 62 seconds into the simulation. The wave prediction algorithm derives the predicted force using the prediction of the vessel velocity, seen in Figure 6. For the MPC with wave prediction the optimal state and control trajectories are then computed considering the waves. As seen in Figure 5a, the optimal state trajectory over the prediction horizon is similar

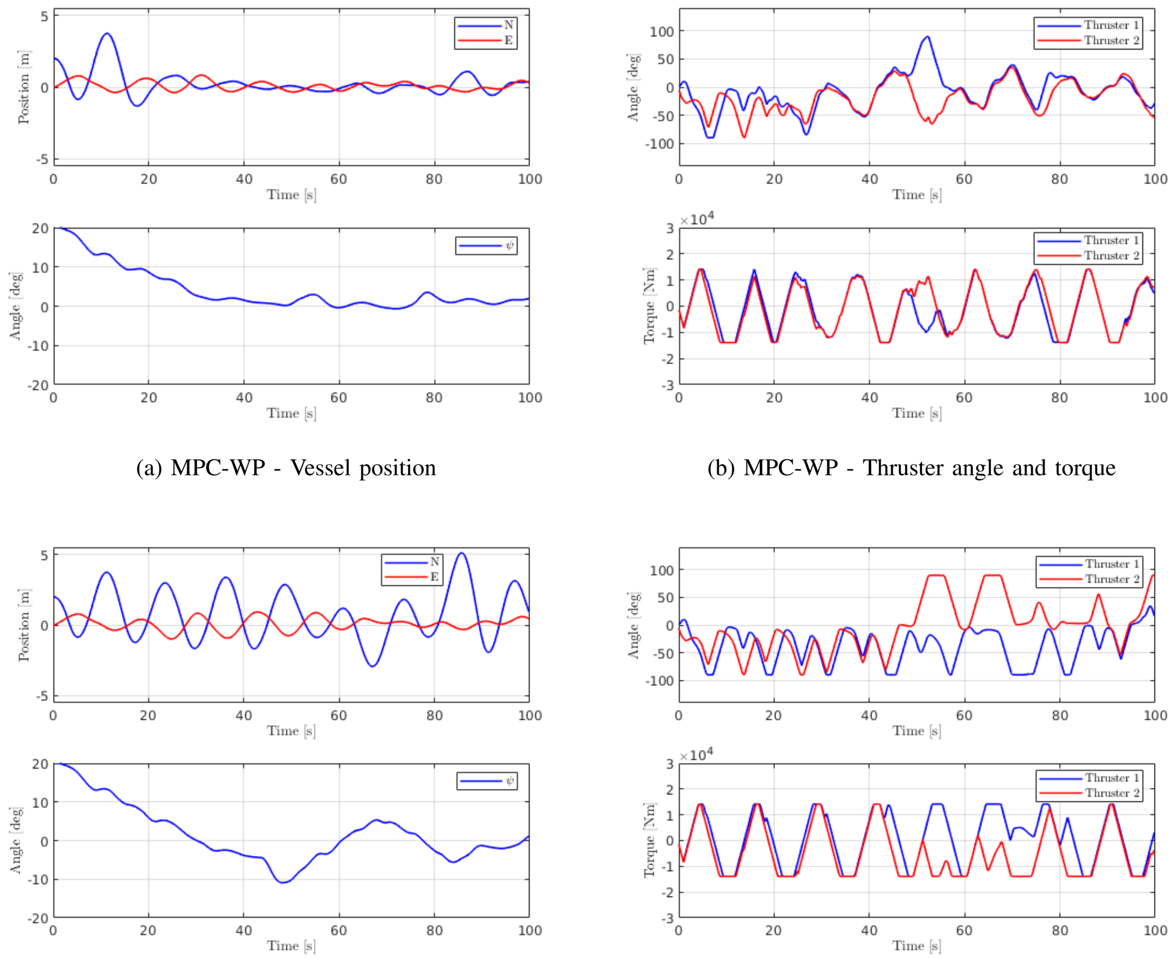

(a) MPC-WP - Vessel position

(b) MPC-WP - Thruster angle and torque

(c) MPC Baseline - Vessel position

(d) MPC Baseline - Thruster angle and torque

Fig. 3. Vessel positions and thruster controls for both controllers in the third scenario.

to the true trajectory the vessel end up taking. This is not the case for the MPC without wave prediction, as demonstrated in Figure 5b, where the optimal state trajectory computed by the controller is very different from the trajectory it ended up taking. The wave prediction contributes to reducing the modelling errors in the controller.

B. Monte Carlo Simulations

The scenarios presented above show a potential benefit of using MPC with prediction with respect to minimizing deviation from the reference point as well as minimizing energy usage. These benefits are dependent on the accuracy of the wave prediction and its ability to correctly predict future wave disturbances based on the previous wave excitation of the vessel. As waves

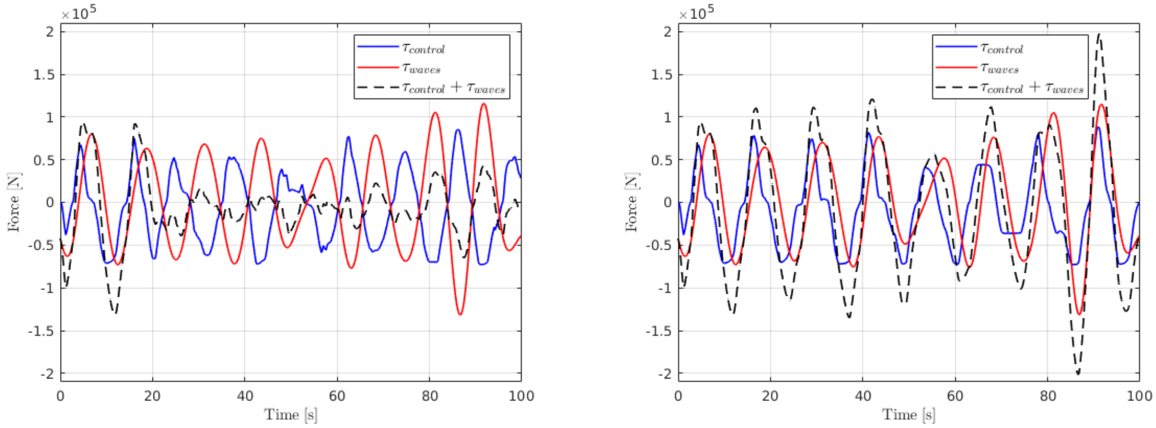

(a) MPC-WP (b) MPC Baseline

Fig. 4. Control forces (blue), environmental forces (red) and the sum of the forces (black) for the simulation in scenario 3.

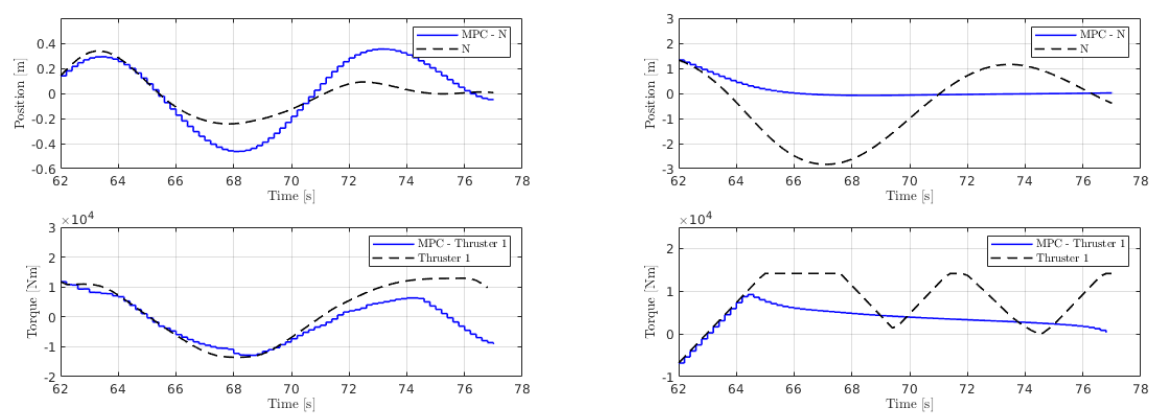

(a) MPC-WP (b) MPC Baseline

Fig. 5. Vessel North position and torque for thruster one as simulated over the prediction horizon in the controller 62 seconds into scenario 3 (blue) and the true position and torque for the future 15 seconds (black).

are stochastic, a Monte Carlo (MC) simulation is performed to evaluate the robustness. Three different sea states are defined based on statistical data from the North sea [23], summarized in Table II. The waves are headed from south to north for all simulations. In addition, a current of 0.3 m/s and with direction 15° is added. For each sea state 40 simulations of 350 seconds with randomly generate waves are run where the initial 50 seconds are removed to account for the settling time of the wave prediction algorithm. The results are displayed in Table III, IV and V.

On average both controllers are able to keep the reference position with reasonable accuracy, shown in the small mean errors. The controllers are able to counteract the constant disturbance

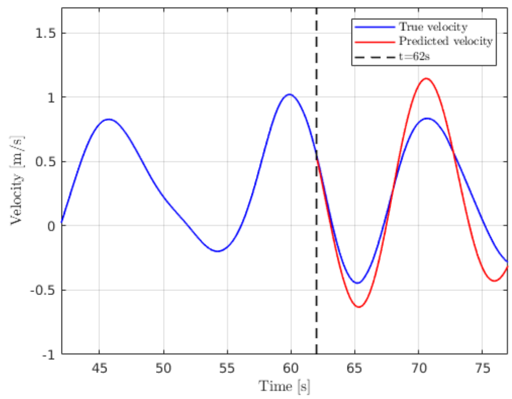

Fig. 6. Predicted and true velocity at 62 seconds into the simulation in scenario 3.

Sea state	Significant wave height	Peak wave period	Wave direction
Slight	$1m$	$6s$	0°
Moderate	$3m$	$9s$	0°
High	$5m$	$12s$	0°

TABLE II

SEA STATES PARAMETERS USING THE JONSWAP SPECTRUM.

MPC with wave prediction	North	East	Yaw
Avg. mean error	$0.011m$	$0.003m$	-0.207°
Avg. RMS error	$0.364m$	$0.249m$	1.326°
Avg. max error	$1.260m$	$0.770m$	4.510°
Avg. NNFD	46.7%	83.9%	248.7%
MPC without wave prediction	North	East	Yaw
Avg. mean error	$-0.095m$	$0.115m$	-0.227°
Avg. RMS error	$1.044m$	$0.356m$	1.967°
Avg. max error	$3.450m$	$1.070m$	6.190°
Avg. NNFD	128.6%	111.0%	297.4%

TABLE III

MONTE CARLO STATISTICS FOR HIGH SEA STATE.

from the current. When it comes to cancel out wave motion and stay as close to the reference point over time the controller with wave prediction significantly outperform the MPC baseline. The average RMS along the north-axis is reduced with 65.6%, 59.6% and 12.7% for high, moderate

MPC with wave prediction	North	East	Yaw
Avg. mean error	$0.001m$	$-0.019m$	$-0.368°$
Avg. RMS error	$0.245m$	$0.180m$	$1.315°$
Avg. max error	$0.880m$	$0.580m$	$4.310°$
Avg. NNFD	55.0%	89.9%	163.7%
MPC without wave prediction	**North**	**East**	**Yaw**
Avg. mean error	$-0.129m$	$0.059m$	$-0.117°$
Avg. RMS error	$0.594m$	$0.240m$	$1.550°$
Avg. max error	$1.940m$	$0.740m$	$5.740°$
Avg. NNFD	120.3%	108.6%	162.2%

TABLE IV

MONTE CARLO STATISTICS FOR MODERATE SEA STATE.

MPC with wave prediction	North	East	Yaw
Avg. mean error	$-0.032m$	$-0.016m$	$-0.042°$
Avg. RMS error	$0.104m$	$0.065m$	$0.990°$
Avg. max error	$0.380m$	$0.220m$	$3.420°$
Avg. NNFD	80.6%	94.4%	126.8%
MPC without wave prediction	**North**	**East**	**Yaw**
Avg. NNFD	83.5%	93.6%	125.2%
Avg. mean error	$0.002m$	$0.049m$	$-0.111°$
Avg. RMS error	$0.130m$	$0.081m$	$0.397°$
Avg. max error	$0.440m$	$0.210m$	$1.290°$
Avg. NNFD	114.2%	103.5%	92.8%

TABLE V

MONTE CARLO STATISTICS FOR SLIGHT SEA STATE.

and slight sea respectively. Along the east-axis the reductions are 30.8%, 27.2%, 14.5%. There is also a significant reduction in the absolute maximum deviation from the reference point, with a reduction as large as 64.1% and 28.7 % along the north- and east-axis for high sea.

The NNFD measures the ratio in RMS between the net external force, that is the sum of the control force and wave forces, and the wave force alone. As the controller will work to cancel out wave forces, the NNFD shows how well the controller is able to reduce first order motion. An example of this is shown in Figure 4 where it can be seen how the net force is significantly closer to zero than the environmental force for the MPC with wave prediction. The average NNFD shows that the MPC with wave prediction is indeed able to reduce the force acting on the vessel for all sea state. The NNFD is reduced to approximately 50% for high and moderate sea and to approximately 80% for slight sea. The MPC baseline controller on the other hand will increase the sum of the external force. In other words the wave motion will be amplified.

C. Discussion

The performance of model-based controllers will naturally depend on the the performance of the model. The simulations shown in the previous section demonstrates a significant increase in accuracy of the DP controller by improving the internal model of the MPC. Regardless of the the desire to counteract first order motion or not, having a model in the MPC that more closely reflect the true dynamics of the vessel will improve the optimally of the controller. In the work demonstrated here the wave prediction clearly improves the controllers ability to counteract first order waves without compromising its ability to act on slowly varying or constant disturbances. By utilizing its control in a more optimal way, e.g., increase the thruster angular velocity ahead of the next wave, the controller improves the position accuracy at the cost of less energy. The MPC baseline controller is successful in acting on the constant disturbance due to current, as has already been demonstrated [11], but fails to act on the disturbance due to first order waves. In fact it is seen in the simulations that the MPC baseline controller will amplify the first order motion. The MPC baseline controller is, similar to more conventional controllers, only able to act on wave induced errors that are observed through the vessel state. Given the constraints on the thrusters and the inertia of the vessel, correcting for a error will take some time as the thrusters will have to rotate and increase or decrease its angular velocity. The high frequency of the waves make the delay significant and results in the thrusters amplifying the wave motion as the force of the waves oscillates as fast as the thruster force can, as seen in Figure 4. The MPC with wave prediction reduces this delay by using the prediction of future waves. In Figure 5 it is shown how MPC with wave prediction correctly predict the arrival of next wave and therefore computes an optimal control trajectory in order to counteract its predicted induced motion. The controller then has more time to increase or decrease thrust. The dynamics of the thruster is therefore an important factor in how well the vessel can counteract first order wave motion. Faster thrusters are likely to further improve the results. However, fast changes in thruster velocity will create larger variations in the onboard electrical load, which again can effect other onboard equipment. Excessive variations in the thruster load can in worst case trigger a blackout onboard where the generators are not able to keep up with the high variation in the electrical load. This is here accounted for by the rate limitation on the torque delivered to the thrusters. Even though the MPC with wave prediction require less energy than the MPC baseline controller, the energy usage is higher than for a more conventional DP controller where PIDs are used in combination with wave filtering techniques [22].

The tuning of the weights of the baseline controller has to reflect the increased modelling error and was here set to be less aggressive compared to the MPC with wave prediction.

The feasibility of the controller is guaranteed with slack variables so that the controller always provides a control action. Is it known that recursively feasible MPC is in general stable, if the prediction horizon is sufficiently large, [31]. In our application, the prediction horizon is 15 seconds, which corresponds approximately to the closed-loop response time of the controller as seen in Figures 1 and 2. It it evident from the theoretical considerations that in this case the neglected tail of the infinite horizon cost-to-go is small, which implies that the conditions for stability are met, which is further verified through simulations.

Sea state	MPC-WP simulation time for 350 seconds	MPC Baseline simulation time for 350 seconds
Slight	621.3s	434.4s
Moderate	631.6s	422.2s
High	623.6s	365.8s

TABLE VI

TIME REQUIRED TO SIMULATE 350 SECONDS WITH THE MPC CONTROLLERS FOR ALL THREE SEA STATES.

A challenge with the MPC approach is the additional computational complexity as a result of solving the nonlinear optimization problem for each time step. For the MPC with wave prediction the second nonlinear optimization problem for finding the model coefficient of the wave model must also be solved. Both problems must be solved online in order to get an optimal control trajectory and thus strict requirements are imposed in a real-time implementation. They can, however, be solved in parallel e.g. on different processing units. The simulation in this study was carried out using MATLAB on a desktop computer and the average required time simulating 350 seconds are shown in Table VI. As the table show, it requires almost two seconds to simulate one second for the MPC with wave prediction. However, as the implementation can be tuned for embedded real-time implementation as described in [32], a real-time implementation is considered feasible. Nonlinear MPC of similar complexity has previously been shown to run in real time on a single board computer onboard a fixed wing Unmanned Aerial Vehicle [33] at much higher update/sampling rates than considered here.

VI. Conclusion

Short-term wave motion prediction combined with model predictive control provides a significant improvement to the positioning of a vessel subjected to wave force disturbances. The controller is able to dampen out some of the zero-mean oscillatory motion caused by first-order wave forces while at the same time counteract slowly varying disturbances. This results in the root mean square error in the position to being reduced with up to 65% compared to controllers where waves are considered unmodelled disturbances. The maximum error is reduced with up to 60% and the root mean square of the wave forces acting on the vessel is reduced with up to approximately 50%, depending on the sea state. The wave prediction integrated into the controller reduce the modelling errors and thus the control trajectories computed are closer to optimal. The dynamics of the thruster system as well as the availability of power is a limiting factor in counteracting first-order waves as the controller will require the thrusters to act dynamically. When the wave frequency increases, the thrusters must be highly dynamic in order to generate the necessary force fast enough.

Acknowledgment

The research is part of the Kongsberg Maritime University Technology Center (UTC) at NTNU, Trondheim. This work was supported by the Research Council of Norway, Kongsberg Martime, Reach Subsea, and DOF Subsea through the ROV Revolution project numbers 296262 and 310166, and the Research Council of Norway, Equinor and DNV GL through the Centre for Autonomous Marine Operations and Systems, project number 223254. Thanks to Reza Firoozkoohi at Sintef Ocean and the team in Kongsberg Maritime for making the hydrodynamic models available.

References

[1] "Rules for classification of ships," DNV GL Std. Part 6 Chapter 3. [Online]. Available: https://rules.dnvgl.com/docs/pdf/DNVGL/RU-SHIP/2019-10/DNVGL-RU-SHIP-Pt6Ch3.pdf

[2] T. Fossen, *Handbook of Marine Craft Hydrodynamics and Motion Control*. Wiley, 2011.

[3] S. Sælid, N. Jenssen, and J. Balchen, "Design and analysis of a dynamic positioning system based on kalman filtering and optimal control," *IEEE Transactions on Automatic Control*, vol. 28, no. 3, pp. 331–339, 1983.

[4] P. Fung and M. Grimble, "Dynamic ship positioning using a self-tuning kalman filter," *IEEE Transactions on Automatic Control*, vol. 28, no. 3, pp. 339–350, 1983.

[5] T. A. Johansen and T. I. Fossen, "Control allocation—a survey," *Automatica*, vol. 49, no. 5, pp. 1087 – 1103, 2013.

[6] A. Veksler, T. A. Johansen, R. Skjetne, and E. Mathiesen, "Thrust allocation with dynamic power consumption modulation for diesel-electric ships," *IEEE Transactions on Control Systems Technology*, vol. 24, pp. 578–593, 2016.

[7] D. Radan, A. J. Sørensen, A. K. Ådnanes, and T. A. Johansen, "Reducing power load fluctuations on ships using power redistribution control," *SNAME Journal of Marine Technology*, vol. 45, p. 162–174, 2008.

[8] E. Mathisen, B. Realfsen, and M. Breivik, "Methods for reducing frequency and voltage variations on DP vessels," 2012.

[9] H. Chen, L. Wan, F. Wang, and G. Zhang, "Model predictive controller design for the dynamic positioning system of a semi-submersible platform," *Journal of Marine Science and Application*, vol. 11, 09 2012.

[10] A. A. do Nascimento, H. R. Feyzmahdavian, M. Johansson, W. Garcia-Gabin, and K. Tervo, "Tube-based model predictive control for dynamic positioning of marine vessels," *IFAC-PapersOnLine*, vol. 52, no. 21, pp. 33 – 38, 2019, 12th IFAC Conference on Control Applications in Marine Systems, Robotics, and Vehicles CAMS 2019.

[11] A. Veksler, T. Johansen, F. Borrelli, and B. Realfsen, "Dynamic positioning with model predictive control," *IEEE Transactions on Control Systems Technology*, vol. 24, pp. 1–14, 2016.

[12] K.-P. Lindegaard, Ph.D. dissertation, Norwegian University of Science and Technology, Trondheim, 2002.

[13] Ø. K. Kjerstad and R. Skjetne, "Disturbance rejection by acceleration feedforward for marine surface vessels," *IEEE Access*, vol. 4, pp. 2656–2669, 2016.

[14] N. Booij, R. C. Ris, and L. H. Holthuijsen, "A third-generation wave model for coastal regions: 1. model description and validation," *Journal of Geophysical Research: Oceans*, vol. 104, no. C4, pp. 7649–7666, 1999.

[15] M. Deo and C. Sridhar Naidu, "Real time wave forecasting using neural networks," *Ocean Engineering*, vol. 26, no. 3, pp. 191 – 203, 1998.

[16] S. Mandal and N. Prabaharan, "Ocean wave forecasting using recurrent neural networks," *Ocean Engineering*, vol. 33, no. 10, pp. 1401 – 1410, 2006.

[17] G. Reikard and W. E. Rogers, "Forecasting ocean waves: Comparing a physics-based model with statistical models," *Coastal Engineering*, vol. 58, no. 5, pp. 409 – 416, 2011.

[18] F. Fusco and J. V. Ringwood, "Short-term wave forecasting for real-time control of wave energy converters," *IEEE Transactions on Sustainable Energy*, vol. 1, no. 2, pp. 99–106, 2010.

[19] F. Fusco and J. Ringwood, "Short-term wave forecasting with ar models in real-time optimal control of wave energy converters," in *IEEE International Symposium on Industrial Electronics*, 2010, pp. 2475–2480.

[20] T. I. Fossen and Ø. N. Smogeli, "Nonlinear Time-Domain Strip Theory Formulation for Low-Speed Manoeuvering and Station-Keeping," *Modeling, Identification and Control*, vol. 25, no. 4, pp. 201–221, 2004.

[21] H. Woud and D. Stapersma, *Design of Propulsion and Electric Power Generation Systems*, ser. IMarEST publications. IMarEST, Institute of Marine Engineering, Science and Technology, 2002.

[22] H. Øveraas, "Dynamic positioning using model predictive control with short-term wave motion prediction," Master's thesis, Norwegian University of Science and Technology (NTNU), Department of Engineering Cybernetics, June 2020.

[23] O. Faltinsen, *Sea loads on ships and offshore structures*. Cambridge University Press, 1990.

[24] *Guide to Wave Analysis and Forecasting*. Secretariat of the World Meteorological Organization, 1998.

[25] A. H. Jazwinski, *Stochastic Processes and Filtering Theory*. Academic Press, San Diego, CA, 1970.

[26] L. Pivano, T. Johansen, and O. Smogeli, "A four-quadrant thrust controller for marine propellers with loss estimation and anti-spin: Theory and experiments," *Marine Technology*, vol. 46, pp. 229–242, 10 2009.

[27] T. I. Fossen and T. Perez, "Marine systems simulator (MSS)," 2004. [Online]. Available: https://github.com/cybergalactic/MSS

[28] WAMIT, "User manual," Available at https://www.wamit.com/manualupdate/v74_manual.pdf (2022/08/31).

[29] J. A. E. Andersson, J. Gillis, G. Horn, J. B. Rawlings, and M. Diehl, "CasADi – A software framework for nonlinear optimization and optimal control," *Mathematical Programming Computation*, vol. 11, no. 1, pp. 1–36, 2019.

[30] A. Wächter and L. Biegler, "On the implementation of an interior-point filter line-search algorithm for large-scale nonlinear programming," *Mathematical programming*, vol. 106, pp. 25–57, 03 2006.

[31] L. Grüne and J. Pannek, *Nonlinear model predictive control*. Springer-Verlag, 2017.

[32] T. A. Johansen, "Toward dependable embedded model predictive control," *IEEE Systems Journal*, vol. 11, pp. 1208–1219, 2017.

[33] D. Reinhardt and T. A. Johansen, "Control of fixed-wing uav attitude and speed based on embedded nonlinear model predictive control," *IFAC-PapersOnLine*, vol. 54, no. 6, pp. 91–98, 2021, 7th IFAC Conference on Nonlinear Model Predictive Control NMPC 2021. [Online]. Available: https://www.sciencedirect.com/science/article/pii/S2405896321013045